A WENO/TVD scheme for the approximation of atmospheric phenomena

Dante Kalise

Dipartimento di Matematica
SAPIENZA-Università di Roma
(joint work with Ivar Lie, StormGeo AS)

14th International Conference on Hyperbolic Problems: Theory, Numerics, Applications
HYP2012, Università di Padova

June 25-29, 2012

SAPIENZA
UNIVERSITÀ DI ROMA

ITN SADCO
Initial Training Network
Sensitivity Analysis for Deterministic Controller Design

Framework

This talk deals with the numerical approximation of two-dimensional systems of balance laws of the form

$$\partial_t Q + \partial_x \mathcal{F}(Q) + \partial_z \mathcal{H}(Q) = \mathcal{S}(Q).$$

The source term is treated via splitting: we solve an advection step

$$\partial_t Q + \partial_x \mathcal{F}(Q) + \partial_z \mathcal{H}(Q) = 0,$$

to be combined with a procedure for the resolution of the source term dynamics

$$\partial_t (Q) = \mathcal{S}(Q).$$

Framework

Ideally, schemes should be:

- Accurate.
- Robust.
- As efficient as possible.

Some schemes in the context of this talk:

- WENO schemes: data reconstruction + low-order flux.
- TVD schemes: monotonicity constraints over reconstructed data.
- WENO/TVD schemes: coherent interaction between non-oscillatory fluxes and high-order reconstructions.

Outline

1. The WENO-TVD scheme
   - High-order of accuracy in space
   - Numerical fluxes
   - High-order of accuracy in time
2. Numerical tests
   - 2D advection
   - 2D convective tests
   - A 2.5D layered model
3. Final remarks

Outline

1. The WENO-TVD scheme
   - High-order of accuracy in space
   - Numerical fluxes
   - High-order of accuracy in time
2. Numerical tests
   - 2D advection
   - 2D convective tests
   - A 2.5D layered model
3. Final remarks

A semi-discrete approach

Averaging in space inside every control volume leads to

Semi-discrete system

$$\frac{dQ_{i,j}(t)}{dt} = -\frac{1}{\Delta x}\left(F_{i+1/2,j} - F_{i-1/2,j}\right) - \frac{1}{\Delta z}\left(H_{i,j+1/2} - H_{i,j-1/2}\right),$$

where

$$Q_{i,j} = \frac{1}{\Delta x}\frac{1}{\Delta z}\int_{x_{i-1/2}}^{x_{i+1/2}}\int_{z_{j-1/2}}^{z_{j+1/2}} Q(x,z,t)\,dz\,dx,$$

$$F_{i+1/2,j} = \frac{1}{\Delta z}\int_{z_{j-1/2}}^{z_{j+1/2}} \mathcal{F}\left(Q(x_{i+1/2},z,t)\right)dz\,,$$

$$H_{i,j+1/2} = \frac{1}{\Delta x}\int_{x_{i-1/2}}^{x_{i+1/2}} \mathcal{H}\left(Q(x,z_{j+1/2},t)\right)dx.$$

Approximated formulation

We approximate the fluxes by conventional Gaussian quadrature formulas

$$F_{i+1/2,j} \approx \frac{1}{2} \sum_{z_{Gp}} w_{z_{Gp}} \mathcal{F}\left(Q(x_{i+1/2}, z_{Gp}, t)\right) dz \,,$$
$$H_{i,j+1/2} \approx \frac{1}{2} \sum_{x_{Gp}} w_{x_{Gp}} \mathcal{H}\left(Q(x_{Gp}, z_{j+1/2}, t)\right) dz \,.$$

In order to compute flux calculations we want:

- High-order accurate values for Q at Gauss points.
- A proper definition of the numerical fluxes F and H.

Outline

1. The WENO-TVD scheme
   - High-order of accuracy in space
   - Numerical fluxes
   - High-order of accuracy in time
2. Numerical tests
   - 2D advection
   - 2D convective tests
   - A 2.5D layered model
3. Final remarks

The high-order in space scheme

Increasing accuracy in space: WENO interpolation

- Generates one polynomial of degree r per volume, $p_i^r(x) = v(x) + O(\delta x^{r+1})$.
- Conservative with respect to the cell averages

$$\frac{1}{meas(Q_i)} \int_{Q_i} p_i^r(x)\, dx = V_i \; .$$

- Keeps control of the oscillations by weighting according to smoothness indicators.

High-order interpolaton

From *[Balsara et al., Journal of Computational Physics, 2007, 2009]*.

2D WENO reconstruction

In a 2D cartesian mesh, given a set of cell averages $\{q_{ij}\}$ we seek a local and minimal polynomial approximation:

$$
\begin{aligned}
q^r_{ij}(\xi,\zeta) = q_0 + q_x P_1(\xi) + q_z P_1(\zeta) &\quad\longrightarrow\quad \text{2nd order}\\
+q_{xx} P_2(\xi) + q_{zz} P_2(\zeta) + q_{xz} P_1(\xi) P_1(\zeta) &\quad\longrightarrow\quad \text{3rd order}\\
+q_{xxx} P_3(\xi) + q_{zzz} P_3(\zeta) &\\
+q_{xxz} P_2(\xi) P_1(\zeta) + q_{xzz} P_1(\xi) P_2(\zeta) &\quad\longrightarrow\quad \text{4th order}
\end{aligned}
$$

$$
P_1(x) = x\,, \qquad P_2(x) = x^2 - \frac{1}{12}.
$$

High-order interpolaton

2D WENO reconstruction

1. We perform a 1D WENO in each direction in order to recover non-mixed terms.
2. We compute mixed terms with a lower resolution 2D stencils.
3. We compute the 2D smoothness indicators and assign equal weights.

2D stencils

Reconstruction in x-direction

$q_{i-1,j+1}$	$q_{i,j+1}$	$q_{i+1,j+1}$
$q_{i-1,j}$	$q_{i,j}$	$q_{i+1,j}$
$q_{i-1,j-1}$	$q_{i,j-1}$	$q_{i+1,j-1}$

2D stencils

Reconstruction in y-direction

$q_{i-1,j+1}$	$q_{i,j+1}$	$q_{i+1,j+1}$
$q_{i-1,j}$	$q_{i,j}$	$q_{i+1,j}$
$q_{i-1,j-1}$	$q_{i,j-1}$	$q_{i+1,j-1}$

1D reconstruction

1D stencils

$$S^1 = \{Q_{-2}, Q_{-1}, Q_0\}, \quad S^2 = \{Q_{-1}, Q_0, Q_1\}, \quad S^3 = \{Q_0, Q_1, Q_2\}.$$

Reconstructed polynomials

$$Q^{(i)}(x) = Q_0^{(i)} + Q_x^{(i)} P_1(x) + Q_{xx}^{(i)} P_2(x) \qquad i = 1, 2, 3.$$

The coefficients are given by

$$\begin{aligned}
S^1 \quad &: \quad Q_x^{(1)} = \frac{-4Q_{-1} + Q_{-2} + 3Q_0}{2}, \; Q_{xx}^{(1)} = \frac{Q_{-2} - 2Q_{-1} + Q_0}{2}, \\
S^2 \quad &: \quad Q_x^{(2)} = \frac{Q_1 - Q_{-1}}{2}, \; Q_{xx}^{(2)} = \frac{Q_{-1} - 2Q_0 + Q_1}{2}, \\
S^3 \quad &: \quad Q_x^{(3)} = \frac{-3Q_0 + 4Q_1 - Q_2}{2}, \; Q_{xx}^{(3)} = \frac{Q_0 - 2Q_{-1} + Q_2}{2}.
\end{aligned}$$

1D reconstruction

Smoothness indicators

$$IS^{(i)} = \left(Q_x^{(i)}\right)^2 + \frac{13}{3}\left(Q_{xx}^{(i)}\right)^2 .$$

WENO weights

$$\omega^{(i)} = \frac{\alpha^{(i)}}{\sum_{i=1}^{3} \alpha^{(i)}}, \quad \alpha^{(i)} = \frac{\lambda^{(i)}}{(\epsilon + IS^{(i)})^r},$$

$\epsilon = 10^{-12}$, $r = 5$, $\lambda^{(1)} = \lambda^{(3)} = 1$, while $\lambda^{(2)} = 100$.
The 1D reconstructed polynomial is given by

$$Q(x) = \omega^{(1)}Q^{(1)}(x) + \omega^{(2)}Q^{(2)}(x) + \omega^{(3)}Q^{(3)}(x).$$

2D stencils

1st stencil for the computation of q_{xy}

$q_{i-1,j+1}$	$q_{i,j+1}$	$q_{i+1,j+1}$
$q_{i-1,j}$	$q_{i,j}$	$q_{i+1,j}$
$q_{i-1,j-1}$	$q_{i,j-1}$	$q_{i+1,j-1}$

2D stencils

2nd stencil for the computation of q_{xy}

$q_{i-1,j+1}$	$q_{i,j+1}$	$q_{i+1,j+1}$
$q_{i-1,j}$	$q_{i,j}$	$q_{i+1,j}$
$q_{i-1,j-1}$	$q_{i,j-1}$	$q_{i+1,j-1}$

2D stencils

3rd stencil for the computation of q_{xy}

$q_{i-1,j+1}$	$q_{i,j+1}$	$q_{i+1,j+1}$
$q_{i-1,j}$	$q_{i,j}$	$q_{i+1,j}$
$q_{i-1,j-1}$	$q_{i,j-1}$	$q_{i+1,j-1}$

2D stencils

4ht stencil for the computation of q_{xy}

$q_{i-1,j+1}$	$q_{i,j+1}$	$q_{i+1,j+1}$
$q_{i-1,j}$	$q_{i,j}$	$q_{i+1,j}$
$q_{i-1,j-1}$	$q_{i,j-1}$	$q_{i+1,j-1}$

Mixed terms for 2D reconstruction

Cross-term formulas

$$
\begin{aligned}
Q_{xz}^{(1)} &= Q_{1,1} - Q_{0,0} - Q_x - Q_z - Q_{xx} - Q_{zz}\,, \\
Q_{xz}^{(2)} &= -Q_{1,-1} + Q_{0,0} + Q_x - Q_z + Q_{xx} + Q_{zz}\,, \\
Q_{xz}^{(3)} &= -Q_{-1,1} + Q_{0,0} - Q_x + Q_z + Q_{xx} + Q_{zz}\,, \\
Q_{xz}^{(4)} &= Q_{-1,-1} - Q_{0,0} + Q_x + Q_z - Q_{xx} - Q_{zz}\,,
\end{aligned}
$$

The corresponding smoothness indicators are given by

$$
IS^{(i)} = 4\left(Q_{xx}^{(i)}\right)^2 + 4\left(Q_{zz}^{(i)}\right)^2 + \left(Q_{xz}^{(i)}\right)^2 .
$$

Outline

1. The WENO-TVD scheme
   - High-order of accuracy in space
   - Numerical fluxes
   - High-order of accuracy in time
2. Numerical tests
   - 2D advection
   - 2D convective tests
   - A 2.5D layered model
3. Final remarks

Numerical fluxes

FLIC approach

$$
\begin{aligned}
F^{FLIC}_{i+1/2,j} &= F^{FORCE}_{i+1/2,j} + \psi_{i+1/2,j}\left(F^{LW}_{i+1/2,j} - F^{FORCE}_{i+1/2,j}\right),\\
F^{FORCE}_{i+1/2,j} &= \frac{1}{2}\left(F^{LW}_{i+1/2,j} + F^{LF}_{i+1/2,j}\right),\\
F^{LF}_{i+1/2,j} &= \frac{1}{2}\left(\mathcal{F}\left(Q^{L}_{i+1/2,j}\right) + \mathcal{F}\left(Q^{R}_{i+1/2,j}\right)\right),\\
&\quad - \frac{1}{4}\frac{\Delta x}{\Delta t}\left(Q^{R}_{i+1/2,j} - Q^{L}_{i+1/2,j}\right),\\
F^{LW}_{i+1/2,j} &= \mathcal{F}\left(Q^{*}_{i+1/2,j}\right),\\
Q^{*}_{i+1/2,j} &= \frac{1}{2}\left(Q^{L}_{i+1/2,j} + Q^{R}_{i+1/2,j}\right)\\
&\quad - \frac{\Delta t}{\Delta x}\left(\mathcal{F}\left(Q^{R}_{i+1/2,j}\right) - \mathcal{F}\left(Q^{L}_{i+1/2,j}\right)\right).
\end{aligned}
$$

Limiters

The function $\psi_{i+1/2,j} = \psi_{i+1/2,j}(r^L_{i+1/2,j}, r^R_{i+1/2,j})$ is a flux limiter.

Flux limiters

SUPERBEE:

$$\psi(r) = \begin{cases} 0 & \text{if } r \leq 0, \\ 2r & \text{if } 0 \leq r \leq \frac{1}{2}, \\ 1 & \text{if } \frac{1}{2} \leq r \leq 1, \\ \min\{2, \phi_g + (1-\phi_g)r\} & \text{if } r \geq 1, \end{cases}$$

$$\phi_g = \frac{1-|c|}{1+|c|},$$

$$r^L_{i+1/2,j} = \frac{e^R_{i-1/2,j} - e^L_{i-1/2,j}}{e^R_{i+1/2,j} - e^L_{i+1/2,j}}, \qquad r^R_{i+1/2,j} = \frac{e^R_{i+3/2,j} - e^L_{i+3/2,j}}{e^R_{i+1/2,j} - e^L_{i+1/2,j}},$$

$$\psi_{i+1/2,j} = \min(\psi(r^L_{i+1/2,j}), \psi(r^R_{i+1/2,j})).$$

Outline

1. The WENO-TVD scheme
   - High-order of accuracy in space
   - Numerical fluxes
   - High-order of accuracy in time
2. Numerical tests
   - 2D advection
   - 2D convective tests
   - A 2.5D layered model
3. Final remarks

Moving forward in time

At a given starting time t^n, we begin by considering the semi-discrete scheme

$$\frac{dQ_{i,j}(t)}{dt} = L_{i,j}(Q),$$

3rd order TVD Runge-Kutta scheme

$$\begin{aligned}
Q_{i,j}^{n+\frac{1}{3}} &= Q_{i,j}^{n} + \Delta t\, L_{i,j}(Q_{i,j}^{n}), \\
Q_{i,j}^{n+\frac{2}{3}} &= \frac{3}{4}Q_{i,j}^{n} + \frac{1}{4}Q_{i,j}^{n+\frac{1}{3}} + \frac{1}{4}\Delta t\, L_{i,j}(Q_{i,j}^{n+\frac{1}{3}}), \\
Q_{i,j}^{n+1} &= \frac{1}{3}Q_{i,j}^{n} + \frac{2}{3}Q_{i,j}^{n+\frac{2}{3}} + \frac{2}{3}\Delta t\, L_{i,j}(Q_{i,j}^{n+\frac{2}{3}}).
\end{aligned}$$

High-order of accuracy in time

Flow chart of the global scheme of approximation

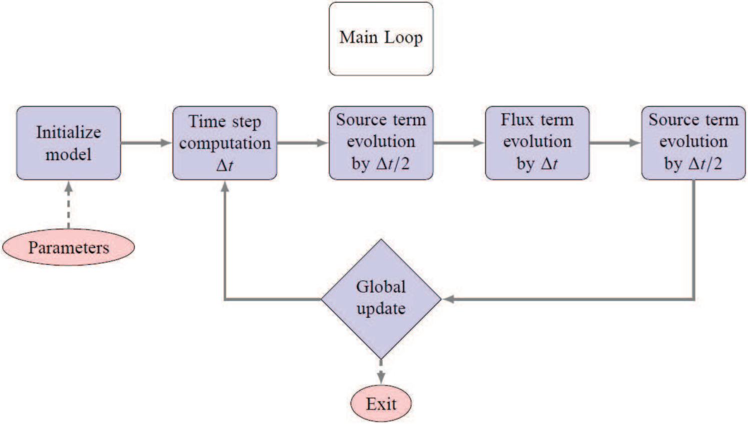

Outline

1. The WENO-TVD scheme
   - High-order of accuracy in space
   - Numerical fluxes
   - High-order of accuracy in time
2. Numerical tests
   - 2D advection
   - 2D convective tests
   - A 2.5D layered model
3. Final remarks

Outline

1. The WENO-TVD scheme
   - High-order of accuracy in space
   - Numerical fluxes
   - High-order of accuracy in time
2. Numerical tests
   - 2D advection
   - 2D convective tests
   - A 2.5D layered model
3. Final remarks

Doswell frontogenesis: setting

We set the domain $\Omega = [-5, 5]^2$, and an advection model given by

$$\partial_t Q + \partial_x (aQ) + \partial_z (bQ) = 0 ,$$

with

$$a = -z f(r), \quad b = x f(r), \quad f(r) = \frac{1}{r} v(r), \quad v(r) = \bar{v}\, sech^2(r)\, tanh(r),$$

$$r = \sqrt{x^2 + z^2}, \quad \bar{v} = 2.59807.$$

The initial condition for this test is given by

$$Q(x, z, 0) = tanh\left(\frac{z}{\delta}\right),$$

generating the following exact solution

$$Q(x, z, t) = tanh\left(\frac{z\cos(vt) - x\sin(vt)}{\delta}\right).$$

Doswell frontogenesis: results

Evolution for a sharp front

Doswell frontogenesis: results

At $t = 4[s]$, for $\delta = 10^{-6}$ and 200×200 elements.

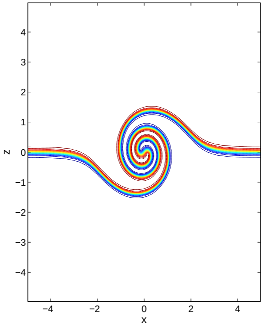

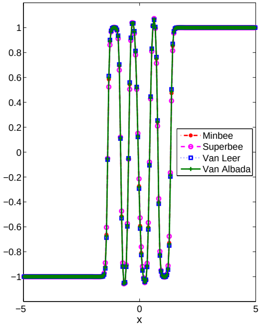

Doswell frontogenesis: results

At $t = 4[s]$, for $\delta = 1$ and 200×200 elements.

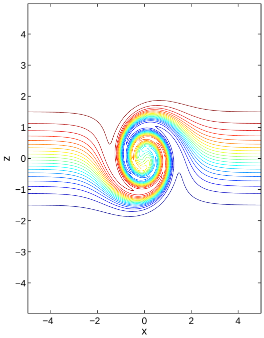

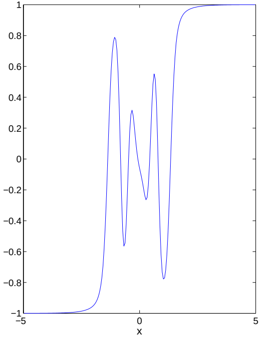

Doswell frontogenesis

Convergence rates at $t = 4$ [s], with $\delta = 1$.

N	L_∞ error	L_∞ order	L_1 error	L_1 order
50	3.4786e-001		1.2719e-002	
100	1.1140e-001	1.6	3.5136e-003	1.9
200	3.3302e-002	1.8	7.3045e-004	2.3
400	5.47780e-003	2.6	1.0541e-004	2.8

Outline

1. The WENO-TVD scheme
   - High-order of accuracy in space
   - Numerical fluxes
   - High-order of accuracy in time
2. Numerical tests
   - 2D advection
   - 2D convective tests
   - A 2.5D layered model
3. Final remarks

The 2D Euler equations

Once the performance of the scheme for space-dependent advection has been assessed, we proceed with further testing for the set of 2D Euler equations

$$\partial_t Q + \partial_x \mathcal{F} + \partial_z \mathcal{H} = \mathcal{S},$$

where

$$Q = \begin{bmatrix} \rho \\ \rho u \\ \rho w \\ \rho\theta \end{bmatrix}, \mathcal{F} = \begin{bmatrix} \rho u \\ \rho u^2 + \mathcal{P} \\ \rho u w \\ \rho u\theta \end{bmatrix}, \mathcal{H} = \begin{bmatrix} \rho w \\ \rho w u \\ \rho w^2 + \mathcal{P} \\ \rho w\theta \end{bmatrix}, \mathcal{S} = -\rho g \hat{k}.$$

The 2D Euler equations

The system is closed by the equation of state for an ideal gas

$$\mathcal{P} = C_0(\rho\theta)^\gamma, \qquad C_0 = \frac{R_d^\gamma}{\mathcal{P}_0^{R_d/c_v}}.$$

Additionally, by defining the Exner pressure π

$$\pi \equiv \left(\frac{\mathcal{P}}{\mathcal{P}_0}\right)^{R/c_p},$$

the expression for the total energy of the system is given by

$$e = E_{Int} + E_{Kin} + E_{Pot} = c_v\theta\pi + \frac{1}{2}(u^2 + w^2) + gz\,.$$

Convective bubble in a neutral atmosphere: setting

The domain is $\Omega = [-10000, 10000] \times [0, 10000]$, with $\Delta x = \Delta z = 125[m]$ and the potential temperature perturbation is given by

$$\theta' = \begin{cases} 2\cos\left(\frac{\pi L}{2}\right) & L \leq 1, \\ 0 & i.o.c. \end{cases}, \quad L = \frac{1}{2000}\sqrt{x^2 + (z-2000)^2}.$$

Simulation time has been set to 1000 [s], allowing the bubble to rise without hitting the top boundary; reflecting solid wall boundary conditions have been considered around the whole domain.

Convective bubble in a neutral atmosphere: results

Potential temperature, $t = 0$, with $\Delta x = \Delta z = 125$[m]

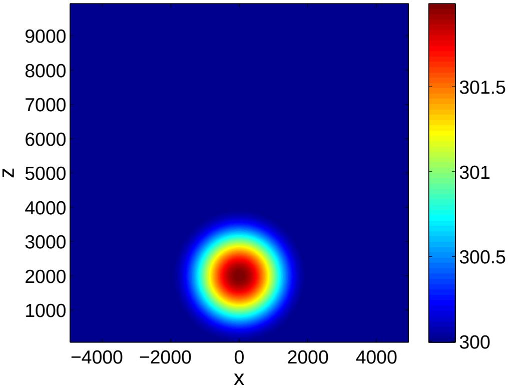

Convective bubble in a neutral atmosphere: results

Potential temperature, $t = 300$, with $\Delta x = \Delta z = 125[\mathrm{m}]$

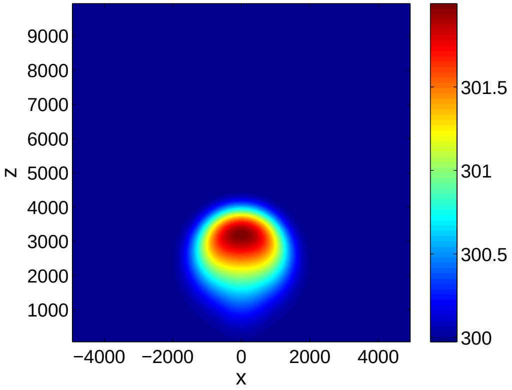

Convective bubble in a neutral atmosphere: results

Potential temperature, $t = 600$, with $\Delta x = \Delta z = 125$[m]

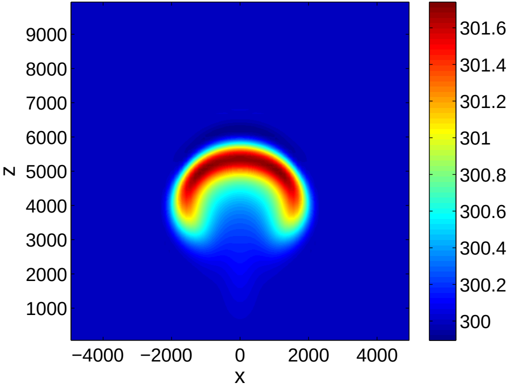

Convective bubble in a neutral atmosphere: results

Potential temperature, $t = 1000$, with $\Delta x = \Delta z = 125[m]$

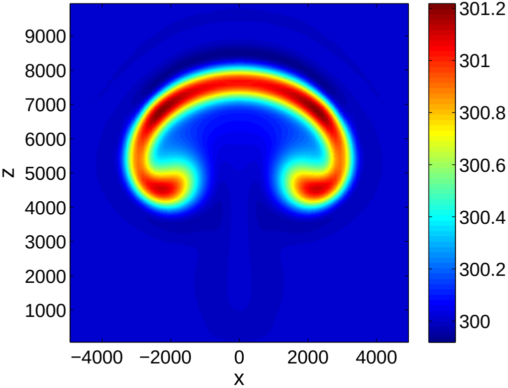

Convective bubble in a neutral atmosphere: results

Normalized energy plot

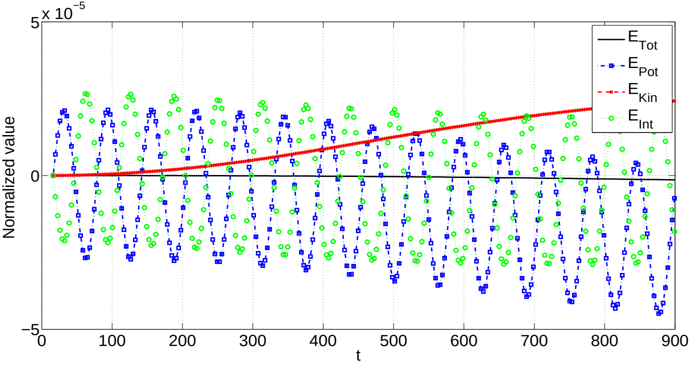

Density current: setting

In the domain $\Omega = [0, 20000] \times [0, 6000]$, with a system initially at rest, a cold bubble perturbation is added to the reference state,

$$\theta' = \begin{cases} -7.5\left(\cos\left(\pi L\right)+1\right) & L \leq 1, \\ 0 & i.o.c. \end{cases}, \; L = \sqrt{\left(\frac{x}{4000}\right)^2 + \left(\frac{z-2000}{2000}\right)^2}.$$

Density current test case: results

Evolution of the perturbation, with $\Delta x = \Delta z = 125[\mathrm{m}]$

Density current: results

Final state after 15 min., $\Delta x = \Delta z = 200$, 100 and 50[m]

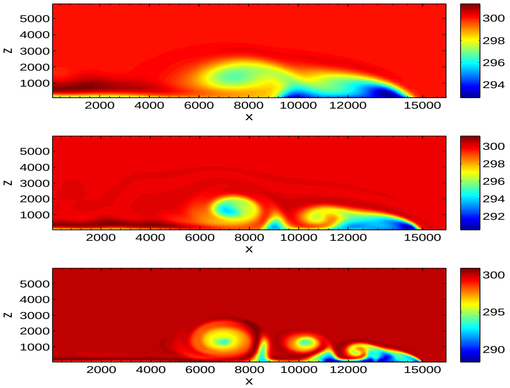

Density current: results

Normalized energy plot

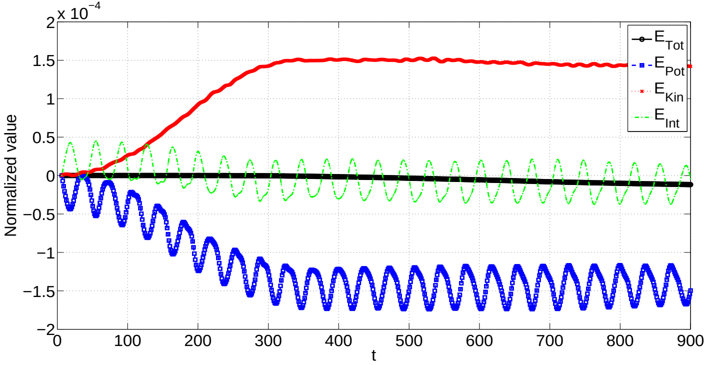

Outline

1. The WENO-TVD scheme
   - High-order of accuracy in space
   - Numerical fluxes
   - High-order of accuracy in time
2. Numerical tests
   - 2D advection
   - 2D convective tests
   - A 2.5D layered model
3. Final remarks

A 2.5D formulation for the Euler equations

1. We consider a set of 3D Euler equations in flux form

$$\partial_t Q + \partial_x \mathcal{F} + \partial_y \mathcal{G} + \partial_z \mathcal{H} = \mathcal{S} \,.$$

2. We introduce 2 layers in the y-direction with a DG procedure.
3. The interface fluxes in the y-direction is approximated taking into account upwind considerations.
4. The dimensionally reduced, 2D system of balance laws

$$\partial_t Q_i + \partial_x \mathcal{F}_i + \partial_z \mathcal{H}_i = \mathcal{S}_i \quad i = 1, 2 \,,$$

is approximated with the previously implemented WENO-TVD scheme.

Interaction between hot and cold bubbles: setting

We set $\Omega = [-10000, 10000] \times [-10000, 10000] \times [0, 10000]$, with $\Delta x = \Delta z = 125[m]$ and Δt chosen according to,

$$\Delta t = CFL \frac{\Delta x}{\max_{i,j} \left(|vel - c_s|, |vel + c_s| \right)},$$

where $CFL = 0.4$, and u is initialized in both layers with a value of $20[ms^{-1}]$. A periodic boundary condition is set in the lateral x-direction while solid boundary walls are kept at the bottom and the top of the domain.

Interaction between hot and cold bubbles: setting

Temperatures in each layer are initialized in a different way:

$$\theta_1 = \bar{\theta}_1 + \theta'_1, \quad \theta_2 = \bar{\theta}_2 + \theta'_2,$$

with

$$\bar{\theta}_1 = \bar{\theta}_2 = 300[K],$$

$$\theta'_1 = \begin{cases} 10\cos\left(\frac{\pi L}{2}\right) & L \leq 1, \\ 0 & i.o.c. \end{cases}, \quad L = \frac{1}{2000}\sqrt{x^2 + (z-2000)^2},$$

$$\theta'_2 = \begin{cases} -15\cos\left(\frac{\pi L}{2}\right) & L \leq 1, \\ 0 & i.o.c. \end{cases}, \quad L = \frac{1}{2000}\sqrt{x^2 + (z-8000)^2}.$$

Hot and cold bubbles: results

Evolution in every layer

Outline

Final comments

Outlook:

- 2D extension of a WENO/TVD scheme.
- Good qualitative and quantitative results in a class of specific problems.

Future research:

- High-order of accuracy.
- Adaptive combination of WENO-TVD.
- Efficiency issues.

Final comments

THANKS FOR YOU ATTENTION!

A WENO/TVD scheme for the approximation of atmospheric phenomena

Dante Kalise

Dipartimento di Matematica
SAPIENZA-Università di Roma
(joint work with Ivar Lie, StormGeo AS)

14th International Conference on Hyperbolic Problems: Theory, Numerics, Applications
HYP2012, Università di Padova

June 25-29, 2012

SAPIENZA
UNIVERSITÀ DI ROMA

ITN SADCO
Initial Training Network
Sensitivity Analysis for Deterministic Controller Design